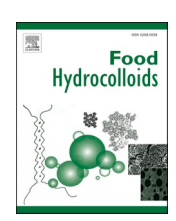
ELSEVIER

Contents lists available at ScienceDirect

# Food Hydrocolloids

journal homepage: www.elsevier.com/locate/foodhyd





# Animal-free scaffold from brown algae provides a three-dimensional cell growth and differentiation environment for steak-like cultivated meat

Heejae Lee <sup>a,b,c,\*\*</sup>, Dasom Kim <sup>a</sup>, Kyeong Hun Choi <sup>a,d</sup>, Sangmin Lee <sup>e</sup>, Minguk Jo <sup>f</sup>, Song-Yi Chun <sup>a</sup>, Yebin Son <sup>a,g</sup>, Jong Ha Lee <sup>a</sup>, Kwanhyeong Kim <sup>a</sup>, TaeByung Lee <sup>a</sup>, Joonho Keum <sup>b,c</sup>, Min Yoon <sup>a</sup>, Hyung Joon Cha <sup>e</sup>, Sangchul Rho <sup>f</sup>, Sung Chun Cho <sup>a,\*\*\*</sup>, Young-Sam Lee <sup>b,c,\*</sup>

- <sup>a</sup> SeaWith Inc., Daegu, 42988, Republic of Korea
- <sup>b</sup> Department of New Biology, DGIST, Daegu, 42988, Republic of Korea
- c Well Aging Research Center, DGIST, Daegu, 42988, Republic of Korea
- <sup>d</sup> Department of Food & Medical Product Regulatory Policy, Dongguk University, Seoul, 04620, Republic of Korea
- <sup>e</sup> Department of Chemical Engineering, Pohang University of Science and Technology, Pohang, 37673, Republic of Korea
- f ANPOLY Inc., Pohang, 37666, Republic of Korea
- g Department of Food Biomaterials, Kyungpook National University, Daegu, 41566, Republic of Korea

#### ARTICLE INFO

# Keywords: Cultivated meat 3D cell culture system ACe-gel (alginate-cellulose hydrogel) scaffold Undaria pinnatifida Bovine muscular stem cell

#### ABSTRACT

Scaffolds for the production of cultivated meat, a promising sustainable meat alternative, should exhibit physical and chemical properties that enable three-dimensional animal cell culture, along with biological characteristics that support cell attachment, proliferation, and differentiation. Additionally, the scaffold should be crafted from edible materials and offer textural similarities to meat and have minimal influence on flavor and taste. Herein, an edible alginate-based alginate-cellulose hydrogel (ACe-gel) scaffold derived from the brown alga Undaria pinnatifida is developed. In terms of physical characteristics, the scaffold had porosity (119.5  $\pm$  37.2  $\mu m$ ) and moisture-holding capacity (73.03  $\pm$  3.82, 68.66  $\pm$  9.54, and 84.17  $\pm$  9.94 at 25 °C, 37 °C, and 60 °C, respectively. tively) suitable for three-dimensional culture and differentiation of boyine muscle stem cells (bMuSCs). Accordingly, the scaffold was superior to a commercial alginate scaffold in terms of the attachment and proliferation of bMuSCs (5.5-fold over 72 h), and its performance was comparable with that of a lyophilized collagen scaffold (7.8-fold over 72 h, compared with the pure alginate). The bMuSCs cultured on the ACe-gel scaffold were capable of differentiating into muscle fibers, as verified by gene expression profile analysis. Furthermore, the scaffold exhibited minimal heavy metal contents and distinct seaweed odorants, while the stress-strain characteristics of the scaffold cultured with bMuSC (Young's modulus of raw ACe-gel:  $285.19 \pm 83.37$  kPa, cooked ACegel meat:  $880.60 \pm 485.60$  kPa) closely resembled that of meat (raw beef:  $267.76 \pm 156.42$  kPa, cooked beef:  $1331.94 \pm 762.43$  kPa). These findings highlight that the seaweed-derived and animal-free ACe-gel scaffold has strong potential for utilization as a food technology for cultured meat production in the future.

#### 1. Introduction

Conventional meat production impacts the environment and animals, which are limited and priceless resources. Meat production processes that do not generate pollution or require the slaughter of animals are needed soon, not only for human survival but also for environmental

sustainability. By 2040, 100 billion more cattle will be needed to produce beef products (Alexandratos & Bruinsma, 2012). To address animal ethics concerns and food shortages, 'cell-based', 'cultured', or 'cultivated' meat is emerging as an alternative food technology (Ben-Arye & Levenberg, 2019; Bhat, Morton, Mason, Bekhit, & Bhat, 2019; Sharma, Thind, & Kaur, 2015; Wheeler & Braun, 2013). However, the

E-mail addresses: leehj9544@dgist.ac.kr (H. Lee), vaga@seawith.net (S.C. Cho), lee.youngsam@dgist.ac.kr (Y.-S. Lee).

https://doi.org/10.1016/j.foodhyd.2024.109944

Received 8 November 2023; Received in revised form 7 February 2024; Accepted 25 February 2024 Available online 26 February 2024

<sup>\*</sup> Corresponding author. Department of New Biology, DGIST, Daegu, 42988, Republic of Korea.

<sup>\*\*</sup> Corresponding author. SeaWith Inc., Daegu, 42988, Republic of Korea

<sup>\*\*\*</sup> Corresponding author.

commercialization of cultivated meat faces challenges such as high production costs and poor sensory qualities, including texture, flavor, taste, aroma, and visual aspects, compared to those of animal-derived meat (Choudhury, Tseng, & Swartz, 2020; Fraeye, Kratka, Vandenburgh, & Thorrez, 2020; van der Weele & Tramper, 2014; Weller, Marley, & Moorby, 2007). To overcome these limitations, the development of materials and methods suitable for commercial-scale culture of the adherent cells that make up meats, including myocytes, is needed.

The primary constituents of meat derived from livestock are bundles of muscle fibers, which contain myofibrillar and sarcoplasmic proteins as the main components (C.-J. Kim et al., 2023; Yan et al., 2022). Consequently, consumption of cultivated meat is not perceived as the ingestion of aggregates of individual cells but rather as the intake of proteins via differentiated muscle fibers. Muscle differentiation involves the transformation of muscle stem cells into myotubes and ultimately into mature muscle fibers. This process is essential for the structural and functional attributes of meat, such as its fibrous texture and the expression of muscle proteins such as myosin and actin. Previous studies determined that there is a significant correlation between the quantity of myosin heavy chain (MHC) and the umami taste, indicating that the existence of appropriately differentiated muscle tissue in cultivated meat is necessary not only as a biological mimetic but also to mimic the flavor, taste, texture, and nutritional aspects of conventional meat (Bomkamp, et al., 2023; Komiya et al., 2020; K. Y. Lee, Loh, & Wan, 2021). Furthermore, the development of systems for thickness-wise muscle cell growth will have a significant impact on the perception of the product as a thick steak-like meat rather than ground meat.

The design of a culture system for this purpose requires simulation of the structure and function of the tissue of interest as well as scalable culture conditions (Haycock, 2011). A three-dimensional (3D) cell culture system can provide a more accurate *in vivo*-like environment than a standard two-dimensional (2D) culture (J. Lee, Cuddihy, & Kotov, 2008). Among the various methods used in 3D cell culture, the scaffold-based method is considered a more effective way to provide a physical space for the adhesion of anchorage-dependent muscle cells and promote alignment of the cells (Jin, et al., 2021; C. H. Li et al., 2022) than scaffold-free methods, such as hanging drops or microfluidic chips (Ianovici, Zagury, Redenski, Lavon, & Levenberg, 2022; MacQueen et al., 2019; Xiang et al., 2022).

Most conventional scaffolds for 3D cell culture are derived from animal materials. However, there are limitations associated with animal-derived scaffolds in that pathogen control and quality assurance are difficult to achieve, and the production cost is considerable (J. Lee, Cuddihy, & Kotov, 2008). On the other hand, most nonanimal-derived scaffolds have limitations in terms of the attachment and growth of adherent cells, requiring complicated modifications (Andersen, Auk-Emblem, & Dornish, 2015; Campuzano & Pelling, 2019; K. Y. Lee & Mooney, 2012; Rowley, Madlambayan, & Mooney, 1999). However, most of these modifications are toxic and expensive, so it is challenging to use the resulting scaffolds for food products. Among other properties, a scaffold used for cultivated meat should be edible and biocompatible.

A 3D cell culture system is also required to adequately diffuse nutrients and oxygen into the inner area during cultivation with a substantial thickness to avoid hypoxia and necrosis. Several studies have attempted to overcome these problems associated with the production of cultivated meat products. For example, spheroids or microtissues with a size that does not cause hypoxia or nutrient depletion have been cultured in studies with the goal of generating meatballs or tissues that resemble meat (Kang, et al., 2021; Liu et al., 2022). Layers of muscle-like or adipose-like tissue have also been reported in the production of cultivated meat (C. H. Li et al., 2022). 3D bioprinting, which is achieved by mixing the cells with photocrosslinkable hydrogels, was applied to manufacture large steak-type cultivated meat products with a sufficient nutrition supply (Jeong, et al., 2022). A scaffold with hollow fibers was introduced to supply nutrients and oxygen within the scaffold (Bomkamp, et al., 2022; Sharma et al., 2015). However, new materials and

techniques for cultivating massive replicates of steak cuts still need to be developed.

Alginate is a polysaccharide composed of β-L-guluronic acid (G-form) and α-D-mannuronic acid (M-form) in a linear copolymer. The majority of commercial alginate comes from brown algae harvested from the sea. Alginate is widely used as a nonanimal-derived material for 3D culture and cellular agriculture because it is biocompatible and has low cytotoxicity (Enrione, et al., 2017; Ianovici et al., 2022; K. Y. Lee & Mooney, 2012). It is also commonly used in food science as a binder, as a stabilizer, in molecular gastronomy, or as a material for imitating food because it is an edible and relatively inexpensive material (Szekalska, Puciłowska, Szymańska, Ciosek, & Winnicka, 2016). However, alginate is limited as a cell culture scaffold because pure alginic acid lacks a domain capable of attaching to animal cells (Andersen, et al., 2015). Although the low cell adhesion capability of alginate is advantageous for cell encapsulation, alginate by itself is not ideal for application in cultivated meat production, which requires the alignment of adherent cells via cell-scaffold interactions rather than cell-cell interactions. To overcome this limitation, cross-linking with Arg-Gly-Asp (RGD) motif-containing peptides or supplementation with animal-origin materials (such as gelatin or collagen) has been introduced to increase cell adhesion to alginate scaffolds (Ianovici, et al., 2022; Rowley et al.,

Phaeophyceae, commonly called brown algae, are marine multicellular organisms belonging to the order Laminariales (Hoek, Mann, Jahns, & Jahns, 1995). Brown algae have the most advanced structure among and play a significant role in the health of marine ecosystems. Anatomically, brown algae have a hypha-like filament network called the trumpet-hypha network in their medullar layer, which functions as a transport channel for photosynthetic metabolites as it exists in the form of a hollow network, similar to a sieve tube in plants (Hoek, et al., 1995; Schmitz & Srivastava, 1976). On a commercial scale, brown algae are a major source of alginate.

In this study, we developed an edible scaffold called alginatecellulose hydrogel (ACe-gel) that is derived from the medulla of brown algae, specifically Undaria pinnatifida (commonly known as miyeok or sea mustard). The polysaccharides, mainly alginate, in the ACe-gel maintain the network structure with nanodots on the surface of the lyophilized scaffolds. In contrast to pure alginate as a conventional non-animal scaffolds, the structural features in the ACe-gel scaffold were utilized to efficiently culture bovine muscle stem cells (bMuSCs) in a 3D environment, demonstrating comparability with the animal-based collagen scaffold. Notably, the ACe-gel provided a cultivation environment with a thickness in the centimeter range for a long period without additional covalent modifications of the scaffold for cell attachment. Furthermore, the differentiated muscle cells were maintained throughout the ACe-gel scaffold as a result of establishing a suitable three-dimensional culture environment. The texture characteristics of the ACe-gel scaffold-based cultivated meat exhibited resilience, cohesion, and springiness comparable to those of beef. This animal-free edible scaffold represents a way to overcome the challenges of commercializing 3D culture approaches.

## 2. Materials and methods

# 2.1. Scaffold fabrication

*U. pinnatifida* was harvested and acquired from a local distributor in Wando, Republic of Korea. Refrigerated seaweeds were washed twice with distilled water to remove debris. The stipes of *U. pinnatifida* were removed with a razor blade. The blades of *U. pinnatifida* were then squeezed with a self-manufactured food squeezer and filtered with a 100 μm mesh filter to extract only the medullar layer without debris from the cortex layer. The ACe-gel, derived from the extracted medullar layer of *U. pinnatifida*, underwent homogenization using a homogenizer (T18 digital ULTRATURRAX; IKA). For comparison purposes, a 2%

alginate solution was prepared by dissolving pure alginate powder (Sigma, A2033) in distilled water, given that the predominant component of the ACe-gel was alginate. Rat-tail collagen (Corning, 354236) was used as a control and neutralized by adjusting the pH with 1 N NaOH. All samples were cast in 24- and 48-well flat-bottom plates (30024, and 30048, respectively; SPL Life Sciences). The casted gels were then frozen at  $-20~^{\circ}\text{C}$  for 24 h and lyophilized using a pilot-scale freeze dryer (LP-20; IlshinBioBase) until the contained moisture was completely removed. For cell seeding, scaffolds were cross-linked using divalent cations in a gelation process with a final concentration of 200 mM Ca $^{2+}$  ions, and the cells were suspended in DMEM. The gelation buffer stock solution was prepared using food-grade CaCl $_2$ ·2H $_2$ O (74% purity; ES food, 186787861).

### 2.2. Structural characteristics of the scaffold

Thermogravimetric analysis utilized a TGA55 instrument (TA Instruments, New Castle, USA), while differential scanning calorimetry was conducted with a DSC25 apparatus (TA Instruments). Fourier-transform infrared spectroscopy was performed using an ALPHA II instrument (Bruker, Billerica, USA), and rheological measurements were carried out with a DHR-10 Rheometer (TA Instruments). All procedures followed protocols detailed in the manufactures' provided references.

For scanning electron microscopy (SEM) sampling of cell-cultured scaffolds, the freeze-drying method reported by Juliana et al. (J. T. Lee & Chow, 2012) was followed. In brief, the cell-cultured scaffold was dried and washed with phosphate-buffered saline (PBS). After glutaraldehyde (GA) fixation, the specimen was rapidly frozen in liquid nitrogen to facilitate physical fixation and freeze-dried for sample preservation. Images were obtained using a scanning electron microscope (JSM-7800F prime, Jeol Ltd., Japan), and pore size was measured using the jPOR plugin in ImageJ software. The porosity of the lyophilized scaffold was measured using AutoPore IV9500 (Micromeritics instrument), and the formula was as follows.

Porosity (%) = 
$$[(D_B - D_A)/D_A] \times 100$$

(D<sub>B</sub>: Bulk density, D<sub>A</sub>: Apparent density)

# 2.3. Quantification of alginate, cellulose, and ash in the ACe-gel

The quantification of alginate in the seaweed and ACe-gel samples was performed using the alkali-soluble alginate (ASA) method. The ground sample was stirred in distilled water at a ratio of 1:20 (w/v) and a temperature of 75  $^{\circ}\text{C}$  for 30 min and filtered with nylon cloth. The residue was mixed with 0.9% Na<sub>2</sub>CO<sub>3</sub> solution at a ratio of 1:20 (w/v) at 75 °C for 4 h. Then, heated distilled water was added to the sample at a ratio of 1:40 (w/v) and filtered with nylon cloth. The filtrate was adjusted to pH 1 with HCl and centrifuged at 1,900×g for 10 min. The supernatant was discarded, and methanol was added to the precipitate at a ratio of 1:20 (w/v). The sample was neutralized at pH 7 with NaOH, filtered using nylon cloth, and dried in a drying oven at 21 °C for 24 h, and then the weight was measured (Nishide, Kinoshita, Anzai, & Uchida, 1988). The extracted sample was prepared for NMR spectroscopy analysis as follows (Jensen, Larsen, & Engelsen, 2015). The alginate extracted from the ACe-gel was dissolved in a hydrochloric acid and ethanol mixture and hydrolyzed under reflux at 100 °C. After ethanol-induced precipitation and drying overnight at 70 °C, the product was reconstituted in D<sub>2</sub>O (1% w/v), filtered through a 0.22 μm Whatman syringe filter, and transferred into an NMR tube. The sample was kept at 90 °C during NMR acquisition.

To quantify cellulose in the ACe-gel, the process started by combining 0.3 g of the ACe-gel scaffold with 3 ml of 72% sulfuric acid for 30 min. Then, the mixture was diluted with water to achieve a 2.5% acid concentration, followed by autoclaving at 121  $^{\circ}\mathrm{C}$  for 30 min. The mixture was neutralized with NaOH, and glucose levels were

determined through the glucose oxidase-peroxidase (GOD-POD) method (Ververis, et al., 2007). The cellulose content was calculated using the formula:

Cellulose (%) = 
$$\frac{0.9 \times C \times V \times \alpha}{0.96 \times M} \times 100$$

(C: glucose concentration, V: solution volume, M: scaffold mass,  $\alpha\textsc{c}$  conversion factor)

For ash residue quantification, the ACe-gel scaffold was first dried at 105  $^{\circ}$ C for 24 h. The dried scaffold sample (0.5 g) was then calcined in a furnace at 575  $^{\circ}$ C for 24 h. The weight of the remaining ash was measured, providing a basis to calculate the ash content percentage.

#### 2.4. Moisture-holding capacity of the lyophilized scaffold

The weights of lyophilized ACe-gel and alginate (each with a dimension of 9.75 mm in diameter and height) were measured using a high-precision scale. The ACe-gel and alginate scaffold were both gels in the presence of 200 mM  ${\rm Ca}^{2+}$ . However, the collagen scaffold was excluded from the measurement of moisture-holding capacity due to its inability to maintain its shape. Subsequently, each scaffold was immersed in distilled water at various temperatures. After a 3-h immersion, the scaffolds were removed, and excess water was removed using blotting paper. The scaffolds were then weighed using a weighing dish. The swelling ratio was calculated according to the equation below.

Swelling ratio = 
$$\frac{W_s - W_d}{W_d}$$

(Ws: Weight of swollen scaffold, Wd: Weight of dried scaffold)

## 2.5. Isolation of bovine muscle stem cells

Primary bovine muscle stem cells (bMuSCs) were provided by Prof. Ki Yong Chung from Korea National College of Agriculture and Fisheries, Jeonju, Korea. Cells were isolated from the semimembranosus (SM) muscle as described in (de Las Heras-Saldana, Chung, Lee, & Gondro, 2019; Kang et al., 2022). To enable the inclusion of biological replicates in the RNA-sequencing analysis, bMuSCs were isolated from three unrelated newborn Korean Hanwoo calves.

# 2.6. Cell proliferation and differentiation in the 3D scaffold

bMuSCs were seeded onto each scaffold at a density of  $4\times10^6$  cells/cm $^3$  to observe cell attachment and proliferation. During the proliferation phase, bMuSCs in scaffolds were incubated in DMEM supplemented with 10% FBS and 100 units/ml penicillin–streptomycin (P/S). For muscle cell differentiation, a sufficient number of proliferated bMuSCs in scaffolds were incubated in DMEM supplemented with 1% FBS, 1  $\mu$ M insulin, and 100 units/ml P/S. All cell cultures were maintained at 37 °C in a 5% CO $_2$  environment. For monitoring metabolic analysis during bMuSC culture in the ACe-gel scaffold. Concentrations of glucose, glutamate, and lactate in the culture media were measured over a week using the Cedex Bio Analyzer (Roche). Media samples were collected at 24-h intervals for analysis.

# 2.7. Cell viability and quantitative measurement of cell growth in the scaffold

Cell viability was evaluated using a Live/Dead Viability/Cytotoxicity kit (Thermo Fisher Scientific, L3224) according to the manufacturer's instructions. To visualize and quantify cell growth, confocal z-stack images were obtained from the samples, with the laser adjusted to an appropriate intensity to prevent any distortion of the cellular volume.

The images were then processed for three-dimensional reconstruction using NIS-Elements software. Within the reconstructed 3D space, the volume occupied by calcein AM was defined as the relative distribution volume. This metric was measured by calculating the total volume of the 3D space filled with the calcein AM fluorescence signal, thus providing a quantitative comparison of cell proliferation within the scaffold.

#### 2.8. RNA isolation

Total RNA was isolated using TRIzol reagent (Invitrogen, 15596026). RNA quality was assessed with a TapeStation4000 System (Agilent Technologies, Amstelveen, The Netherlands), and RNA quantification was performed using an ND-2000 spectrophotometer (Thermo Inc., DE, USA).

#### 2.9. Library preparation and sequencing

Library construction from total RNA and subsequent sequencing of the corresponding cDNA was performed using a NovaSeq 6000 (Illumina Inc., USA) by Ebiogen Inc. (Seoul, Korea). Data mining and graphic visualization were performed using ExDEGA (Ebiogen Inc., Korea).

#### 2.10. Immunofluorescence staining

Cell culture samples were fixed using 4% paraformaldehyde for 24 h at 4 °C. Blocking and permeabilization were performed using 0.5% Triton X-100, 2% BSA, and 10% heat-inactivated horse serum in Dulbecco's phosphate-buffered saline (DPBS) and incubated overnight at 4 °C. Anti-Desmin (Abcam, ab8592), anti-MHC (Millipore, M1570), and anti- $\alpha$ -actinin (Sigma, A7811) antibodies were diluted at a 1:200 ratio in DPBS and incubated for 2 days at 4 °C. After washing the samples three times with 0.025% X-100 in DPBS, Alexa 488-conjugated anti-rabbit (Invitrogen, A11034) and Alexa 594-conjugated anti-mouse (Invitrogen, A11005) secondary antibodies were diluted at a 1:500 ratio in DPBS and incubated with the samples for 1 day at 4 °C, followed by the same washing procedure. 4′,6-diamidino-2-phenylindole (DAPI) staining was carried out with a DAPI-containing fluorescent mounting solution (Abcam, ab104139) and incubated for 30 min in the dark. Finally, the samples were imaged using a confocal microscope.

# 2.11. Reverse transcription-quantitative polymerase chain reaction (RT-qPCR) analysis

cDNAs were generated from the total RNAs using a Maxima First Strand cDNA Synthesis Kit for RT–qPCR (Thermo Scientific), following the manufacturer's instructions. For qPCR, reaction samples were prepared using KAPA SYBR FAST qPCR Master Mix (2×) Universal (Roche). The qPCRs and real-time analyses were performed using a QuantStudio 3 Real-Time PCR System (Applied Biosystems). Information about the primers used in the present study is provided in the Supplementary Information (Supple. Table S1).

# 2.12. Mechanical properties

Texture profile analysis (TPA) was performed using a texture analyzer (TA. XT PLUS100C, Stable Micro System, England) controlled by Texture Exponent software. To measure the force produced by the samples, 100 kg of the load cell was used. To determine the initial contact between the compression plates and the sample, a 5 g load threshold was used. During loading, the machine crosshead moved downward (to compress the sample) at 0.1 mm/s until 50% of its original length was reached. When the maximum deformation was reached, the movement was inverted at a constant speed (0.1 mm/s) to the original position. After a 5-s pause, another cycle was performed. The stress-distance curve was obtained using the representative values closest to the average modulus values for each sample. In this process,

the variation in distance among samples was corrected by applying a factor that accounted for the inherent difficulty of exactly matching the sizes of all samples before and after testing. A compression test was performed on all samples under the same strain rate. Based on this, the average modulus values between 0 and 2 s were obtained, and the corrected compressive modulus was computed by applying a factor to compensate for variations in volume among the samples.

#### 2.13. Volatile compound profiling with an electronic nose

The fast GC e-nose Heracles Neo (Alpha M.O.S., France) with two hydrogen flames (FID) was used for analysis. The AroChemBase (Alpha M.O.S., France) library, which is a program installed on the device, was used to confirm identification. The analysis conditions were as follows: injection volume, 5,000  $\mu$ l; injection speed, 125  $\mu$ l/s; and initial temperature of the search trap, 35 °C.

#### 2.14. Statistical analysis

All experiments were conducted a minimum of three times to ensure statistical significance. Data were analyzed using GraphPad Prism (GraphPad Software, CA, USA) and are presented as the means  $\pm$  standard deviations (SD). Statistical comparisons were made using one-way ANOVA and Tukey's tests, with significance thresholds set at \*p < 0.05, \*\*p < 0.01, \*\*\*p < 0.001, \*\*\*\*p < 0.001, and differences were deemed not significant (n.s.) at p > 0.05.

#### 3. Results

# 3.1. Brown algae-derived nonanimal scaffolds provide a porous microenvironment

As a nonanimal scaffold for a 3D culture system, particularly with the aim of producing cultivated meat, the ACe-gel scaffold with a hyphal network was selectively extracted from the blade of *U. pinnatifida* (Fig. 1A–C). Notably, the ACe-gel was able to be fabricated to a thickness in the centimeter range, which is required for the application of the scaffold for the production of steak-like cultivated meat (Fig. 1D).

To identify the chemical properties suitable for cell culture in the fabricated hydrogel scaffold, the main components constituting the scaffold were firstly analyzed. Macroalgae contain many polysaccharides, including predominantly alginate, as well as others, such as cellulose and fucoidan (Bar-Shai, Sharabani-Yosef, Zollmann, Lesman, & Golberg, 2021; Koo, 2020; Szekalska et al., 2016). Based on the alkali-soluble alginate (ASA) method (Nishide, et al., 1988), the ACe-gel contained 63.44  $\pm$  2.67% alginate, compared to the value of 40.07  $\pm$ 4.00% for *U. pinnatifida* (Fig. 2A). Meanwhile, it was determined that cellulose constituted 1.01  $\pm$  0.06% in the ACe-gel, while ash (representing the inorganic salts and minerals) content was found to be 20.75  $\pm$  0.56% (Supple. Fig. S1). The previously reported contents of cellulose and ash in *U. pinnatifida* are approximately 20% and 25%, respectively (Im, Choi, & Kim, 2006; Rupérez & Saura-Calixto, 2001). The difference in alginate and cellulose content between the ACe-gel and its source may be due to the removal of the cortex composed of dense cells in the brown algae during the fabrication process of the scaffold. The detected cellulose is also expected to be derived from the thin hyphal network. These findings indicate that the ACe-gel scaffold is a composite material predominantly composed of a substantial amount of alginate.

When transforming an alginate solution into a hydrogel through cross-linking, the physical strength of the resultant scaffold is determined by the proportion of M-form over G-form (M/G ratio) residues of alginate, in that G-form residues in different chains of alginate polymers have been cross-linked by divalent cations, most commonly Ca<sup>2+</sup> (K. Y. Lee & Mooney, 2012). Previous studies have shown that alginate with a higher proportion of the M-form than the G-form (a higher M/G ratio) improves cell proliferation (Stabler, Wilks, Sambanis, & Constantinidis,

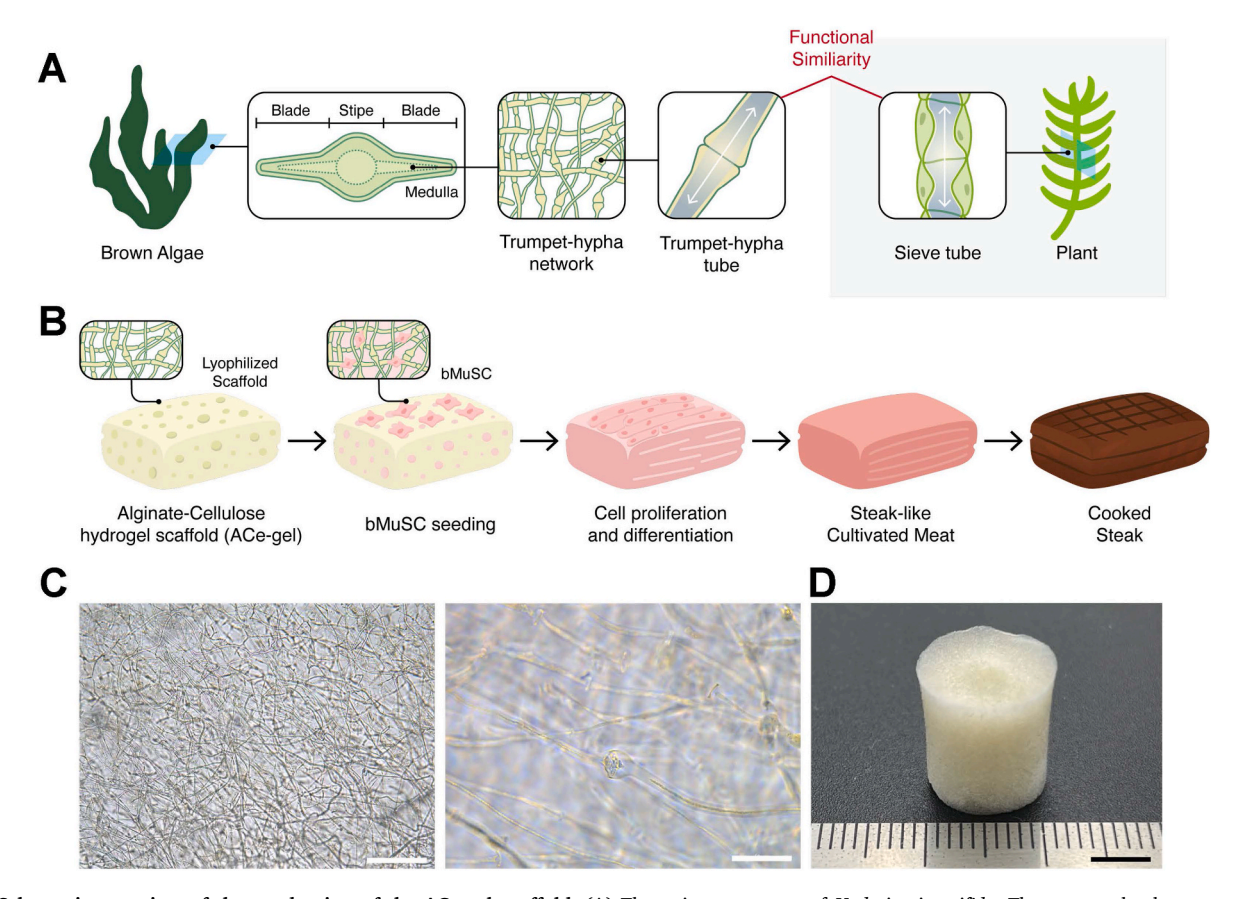


**Fig. 1. Schematic overview of the production of the ACe-gel scaffold.** (A) The unique structure of *Undaria pinnatifida*. The trumpet-hypha structure in the medullar layer of brown algae functions like the sieve tube of a plant. (B) Manufacture process of the ACe-gel scaffold and its application to generate steak-like cultivated meat. (C) Optical microscope images of a trumpet-hypha network of *U. pinnatifida* (left) and magnified image of trumpet-hypha (right). Scale bars: 500 μm (lower magnification) and 50 μm (higher magnification). (D) The ACe-gel scaffold with a thickness of 1 cm. Scale bars: 5 mm.

2001). The M/G ratio of ACe-gel measured by NMR spectroscopy was 1.3788, indicating a higher proportion of the M-form than G-form residues (Supple. Fig. S2); this shows that the ACe-gel can provide favorable conditions for cell proliferation.

To characterize the chemicophysical properties of the ACe-gel, the following analyses were employed: thermogravimetry (TGA), differential scanning calorimetry (DSC), Fourier transform infrared spectroscopy (FT-IR), rheo-modulus and rheo-viscosity. TGA analysis showcased significant events in the ACe-gel's behavior. At 43.11 °C (point 1 on Supple. Fig. S3A), a peak change attributed to the evaporation of trapped water was observed. Additionally, at 240.28 °C, a peak change due to polymer degradation was identified (point 2 on Supple. Fig. S3A). This aligns with the expected decomposition pattern of alginate, reinforcing the notion of the alginate backbone structure undergoing degradation (Estrada-Villegas, Morselli, Oliveira, Gonzalez-Perez, & Lugão, 2020; Salisu et al., 2016). Differential scanning calorimetry (DSC) analysis provided corroborating evidence, revealing an endothermic event related to water vaporization at 119.72 °C (point 1 on Supple. Fig. S3B) and a subsequent peak change due to polymer degradation at 247.24 °C (point 2 on Supple. Fig. S3B) (Fajardo, et al., 2012).

FT-IR analysis offered further insights into the ACe-gel's composition. Peaks at 3264 cm<sup>-1</sup> (O–H stretching), 2920 cm<sup>-1</sup> (C–H stretching), 1601 cm<sup>-1</sup> (asymmetric stretching of carboxylate anions), 1405 cm<sup>-1</sup> (symmetric stretching of carboxylate groups), and 1030 cm<sup>-1</sup> (C–O stretching vibrations) strongly resembled the typical FT-IR signature of alginate (Supple. Fig. S3C) (Estrada-Villegas, et al., 2020; Fajardo et al., 2012; Salisu et al., 2016). This collective presence of characteristic peaks strongly supports the conclusion that alginate is a predominant

component within the ACe-gel scaffold.

The rheo-modulus profile of the ACe-hydrogel exhibited a higher storage modulus (G') compared to the loss modulus (G''), indicative of its predominantly elastic properties over viscous ones (Supple. Fig. S3D). The moduli displayed a slight increase with frequency, suggesting the hydrogel's persistent solid-like behavior. The rheo-viscosity graph showed viscosity reduction as shear rate increased, indicating shearthinning behavior (Supple. Fig. S3E). This result suggests that the hydrogel can align and flow more readily under applied stress, a property advantageous for its processing and application in tissue engineering.

Next, the essential physical properties for 3D cell culture, including the pore size, porosity, and moisture-holding capacity of the lyophilized scaffolds, were analyzed. For comparison of the ACe-gel with conventional 3D culture scaffolds, alginate scaffolds, representing non-animalbased materials, and collagen scaffolds, which are animal-based materials, were used in the following experiments. A high moisture-holding capacity, as represented by the swelling ratio (the weight of water retained by the lyophilized scaffolds relative to their weight), is an important physical property in 3D cell culture, as it exerts a positive effect on initial cell attachment and proliferation and facilitates nutrient exchange (Jithendra, Rajam, Kalaivani, Mandal, & Rose, 2013; J. Li et al., 2020). We assessed the swelling ratio after soaking the scaffolds in water for an extended time (3 h) at various temperatures by simulating a cooking process of cultivated meat. The swelling ratio of the ACe-gel scaffold was more than two times greater than that of the alginate scaffold (ACe-gel scaffold: 73.03  $\pm$  3.82, 68.66  $\pm$  9.54, and 84.17  $\pm$ 9.94 at 25 °C, 37 °C, and 60 °C, respectively; alginate scaffold: 33.20  $\pm$ 3.59, 32.23  $\pm$  1.51, and 45.57  $\pm$  8.13 at each temperature,

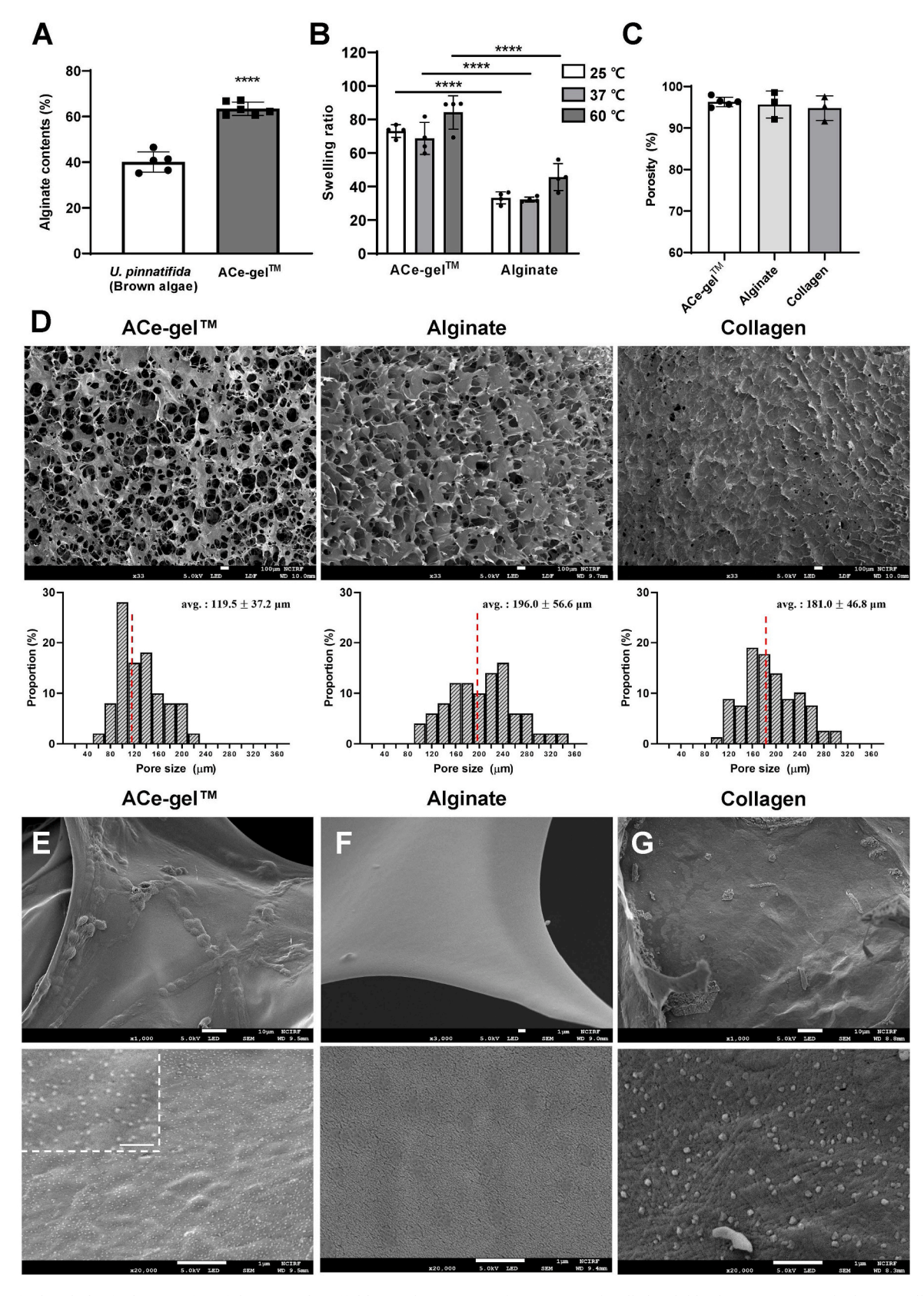


Fig. 2. Chemical and physical properties of the ACe-gel scaffold. (A) Alginate quantification using the alkali-soluble alginate (ASA) method. (B) Swelling ratio of the ACe-gel and alginate scaffold. (C) Porosity of the lyophilized ACe-gel, alginate, and collagen scaffolds. (D) Scanning electron microscopy (SEM) images and pore size distribution of the lyophilized ACe-gel, alginate, and collagen scaffolds. (E–G) High-magnification images at  $1,000 \times \text{(upper, scale bar: } 10 \, \mu\text{m})$ ,  $20,000 \times \text{(lower, scale bar: } 1 \, \mu\text{m})$ , and dotted box (scale bar: 250 nm). SEM images of the surface of the lyophilized ACe-gel (left), alginate (middle), and collagen (right) scaffolds.

respectively), demonstrating the stable water-retention capacity of the ACe-gel scaffold even as the temperature increased (Fig. 2B). Both scaffolds exhibited a slight increase in swelling ratio values at 60 °C, which might be due to structural decomposition of the scaffolds at higher temperatures. Of note, the collagen scaffold was excluded from this assay because it failed to maintain structural stability during hydration in the buffer, leading to dissolution and preventing accurate measurement.

Porous structures in scaffolds for 3D cell culture are essential for the transport of oxygen and nutrients to the interior region of the scaffold and the efficient removal of metabolic wastes. Generally, a pore size range of 50  $\mu m$ -200  $\mu m$  supports effective cell growth and tissue formation (M. Lee, Wu, & Dunn, 2008; Zeltinger, Sherwood, Graham, Müeller, & Griffith, 2001). The porosity of lyophilized scaffolds assessed using a porosimeter was over 90% for all tested scaffolds, which is known to facilitate sufficient diffusion and 3D tissue formation (Freed, et al., 1994; M. Lee, Cuddihy, & Kotov, 2008) (Fig. 2C). Interestingly, based on scanning electron microscopy (SEM) images, the ACe-gel scaffold showed an average pore size of 119.5  $\pm$  37.2  $\mu m$ , which is smaller and has a narrower deviation than the alginate (196.0  $\pm$  56.6  $\mu$ m) or collagen (181.0  $\pm$  46.8  $\mu$ m) scaffold, indicating that the ACe-gel creates a more uniform environment for 3D cell culture than other conventional 3D scaffolds (Fig. 2D). In connection with the porosity of the scaffold, 40 kDa fluorescein isothiocyanate (FITC)-labeled dextran was uniformly distributed into the interior of the gelated ACe-gel scaffold with a height of 5 mm within 10 min (Supple. Fig. S4).

Unexpectedly, high-magnification SEM images of the ACe-gel showed a distinct distribution of 20 nm-sized nanodots on the surface of the lyophilized scaffolds, which was not observed for the alginate scaffold (Fig. 2E and F, Supple. Fig. S5A). In the collagen scaffold, nonuniform particles with sizes of several hundred nanometers were observed. However, in contrast to the ACe-gel scaffold with 20 nm-sized nanodots, the collagen scaffold particles, being on the scale of hundreds of nanometers, are typically not considered to have nanotopographical characteristics (Fig. 2G). Energy-dispersive spectroscopy (EDS) determined that the nanodots were composed of sodium alginate (Sun, et al., 2020) (Supple. Fig. S5B). The average nearest-neighbor distance between nanodots was 58.3  $\pm$  22.1 nm (Supple. Fig. S5A). In terms of nanotopography, it has been reported that the spacing of nanodots affects cell adhesion (Arnold, et al., 2004; Ben-Arye, et al., 2020), indicating that, unlike other scaffolds, the ACe-gel might allow for cell-scaffold interactions in a highly uniform and dense manner via

The physicochemical properties of the scaffold, including surface hydrophobicity and charge, impact cell behavior. Therefore, the characteristics of the scaffolds were assessed through contact angle and zeta potential measurements. The ACe-gel scaffold displayed a contact angle indicative of hydrophilicity, with all scaffolds exhibiting angles below 90° (Supple. Fig. S6A). Regarding surface charge, collagen exhibited a neutral charge, as indicated by its zeta potential approaching zero. Interestingly, despite the ACe-gel's alginate-based composition, its zeta potential was less negative than that of pure alginate (Supple. Fig. S6B). This variation in zeta potential could potentially contribute to the superior cell culture performance of the ACe-gel scaffold compared to conventional alginate.

# 3.2. The ACe-gel scaffold provides a suitable environment for cell adhesion and proliferation

To verify whether the ACe-gel scaffold can provide an environment for muscle cells to attach and proliferate under 3D conditions that are comparable to that provided by other scaffolds (alginate and collagen), bMuSCs were seeded onto scaffolds and observed for 3 days. Scaffolds were maintained under lyophilized conditions before seeding cells to ensure uniformity of the cell culture conditions. For the collagen scaffold, 3D printed anchors were employed to maintain a uniform volume

and prevent shrinkage over time (Supple, Fig. S7). At 24 h after cell seeding, there were no discernible differences in the relative distribution volume across all three scaffold groups (Fig. 3A and B), indicating that the initial cell distribution in each scaffold was reliable and homogeneous. The seeding efficiency of bMuSCs in the ACe-gel scaffold was more than 95% (Supple. Fig. S8). Notably, cells within the ACe-gel and alginate scaffolds showed a spheroid-like cell morphology compared with single cells dispersed within the collagen scaffold. At 48 h after cell seeding or later, the cells in the ACe-gel scaffold were highly proliferative and exhibited a bipolar, elongated cell morphology that resembled fibroblasts in a 2D culture environment, indicating that the cells in the ACe-gel scaffold could stably interact with the scaffold (Fig. 3A and B). The cell morphology and proliferation results were similar to those obtained with the collagen scaffold. However, the alginate scaffold did not significantly increase the number of cells, and the morphology of the cells was restricted to a spheroid-like form, suggesting that the alginate scaffold provides an environment suitable for cell-cell interactions rather than cell-scaffold interactions (Fig. 3A and B).

Interestingly, the fibrous network structure of the ACe-gel could be visualized with the saturated ethidium homodimer-1 (EthD-1) signal after the Live/Dead assay. This is because the scaffold did not undergo a separate decellularization process with detergents (e.g., sodium dodecyl sulfate), and as a result, some nucleic acid fragments remaining in the brown algae reacted with EthD-1. This feature was adapted to observe the detailed interaction between cells and the ACe-gel scaffold. The results of the live/dead assay after seeding bMuSCs showed that the cells were aligned with the network of the scaffold (Fig. 3C). Furthermore, SEM imaging of the scaffold in which bMuSCs were cultured for two days showed that the cells were effectively attached and interacted with the scaffold (Fig. 3D). Notably, cells adhered throughout the centimeter thickness of the scaffold when observed three day after seeding (Supple. Fig. S9). These results collectively demonstrated that the ACe-gel scaffold provides a suitable environment for the adhesion and proliferation of bMuSCs. Regarding the production quality control to ensure the experimental reproducibility of using the ACe-gel scaffold, viscosity of the extract from *U. pinnatifida* was identified as crucial. It was found that when viscosity falls below 1,000 cp, cell-scaffold interactions decrease, leading to reduced cell culture efficiency. While an increase in viscosity does not significantly affect cell culture, excessively high viscosity is discouraged as it decreases production efficiency. Based on these findings, only products with a viscosity in the range of 1,200 to 2,500 cp are utilized for cell culture (Supple. Fig. S10).

### 3.3. bMuSCs successfully differentiated on the ACe-gel scaffold

In 3D culture for the production of cultivated meat, the differentiation of muscle stem cells into mature myocytes is essential to form muscle fibers, as shown in animal meat. To validate that the ACe-gel scaffold provides an environment for differentiation, we first monitored morphological changes in the bMuSCs in the ACe-gel after inducing insulin-mediated muscle differentiation. After 8 days in the insulin-containing differentiation medium, the cells at high density exhibited myotube-like morphologies (Fig. 4A). The results of immunofluorescence staining confirmed that desmin and myosin heavy chain (MHC), muscle differentiation markers, were highly expressed in the myotube-like cells after 8 days in the differentiation medium (Fig. 4B and C). In addition, the mRNA expression of muscle differentiationrelated genes, including myogenin, MHC1, and MHC2A, was upregulated after the induction of muscle differentiation conditions. Notably, cells cultured in the ACe-gel-based 3D condition presented higher mRNA expression of these muscle differentiation markers than cells cultured in a conventional monolayer with the corresponding differentiation medium for 8 days (Fig. 4D).

The transition from a proliferation medium, rich in essential nutrients for muscle cell proliferation, to a low-serum medium for muscle differentiation raised concerns about potential nutrient deficiencies that

Food Hydrocolloids 152 (2024) 109944

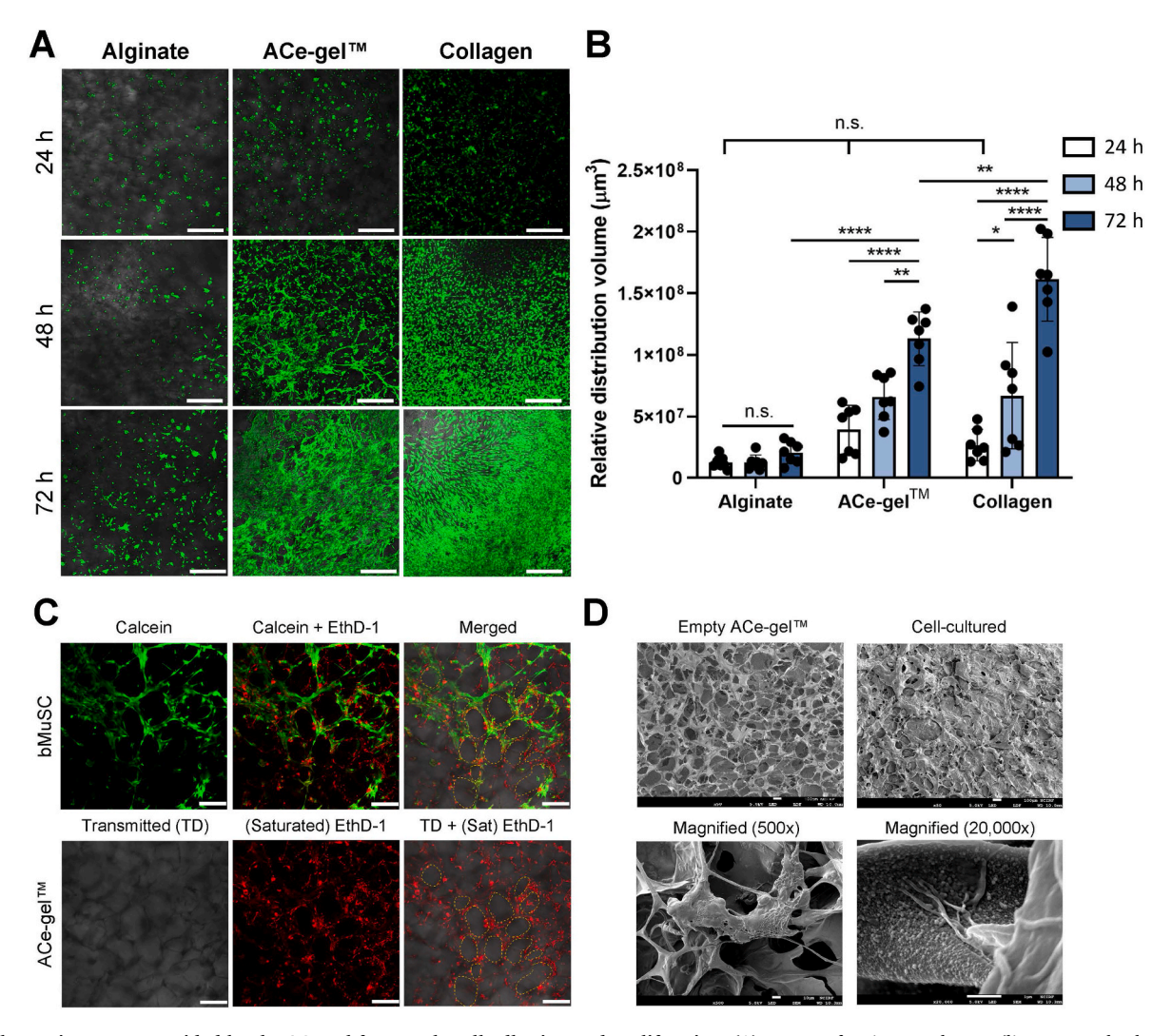


Fig. 3. The environment provided by the ACe-gel for muscle cell adhesion and proliferation. (A) Images of a Live/Dead assay (live; green, dead; red) of cells cultured on the alginate, ACe-gel, and collagen scaffolds for 72 h. Images were obtained using a confocal microscope with a 200 μm z-stack. Scale bar: 500 μm. (B) Relative distribution volume of live cells in the 3D position in each scaffold. Image based quantification was applied to measure the distribution volume of live cells within the scaffold. (n.s. > 0.05, \*p < 0.05, \*p < 0.01, \*\*\*p < 0.001, and \*\*\*\*p < 0.0001) (C) Confocal microscopy images of cell-free scaffolds and cell-cultured scaffolds. bMusCs were aligned with the network composed of trumpet-hypha. Scale bar: 200 μm. (D) SEM images of bMusCs cultured with the ACe-gel scaffold. Empty ACe-gel scaffold (upper left, scale bar: 100 μm), cell-cultured ACe-gel scaffold (upper right, scale bar: 10 μm), and magnified image of cells on the surface of the scaffold (lower).

could compromise the culture environment. To address this, metabolic analysis was conducted over a week of differentiation in two groups: one cultured without changing media and another with media changed every two days. Confocal microscopy images revealed that cells in both groups proliferated and differentiated similarly, maintaining adequate glucose levels throughout the week (Supple. Figs. S11A and B). Metabolite analysis indicated continuous production of metabolites such as glutamate and lactate throughout the differentiation process. Particularly, in the group with unchanged media, the levels of glutamate and lactate gradually increased but remained below threshold that could adversely affect cell viability (Lin, et al., 2017; Tsai, Jeske, Chen, Yuan, & Li, 2020; Yang et al., 2019). In contrast, the group with media changes every two days showed efficient removal of these metabolites (Supple. Figs. S11C and D). Overall, these results indicate that the induction of bMuSCs' differentiation can proceed without the need for media replacement, which is an important consideration for reducing the costs of cultivated meat production. Furthermore, these results suggest that the ACe-gel provided a 3D environment for muscle cell differentiation.

3.4. mRNA profiling reveals the ACe-gel scaffold's superiority in muscle cell differentiation over alginate and collagen scaffold

To elucidate the detailed molecular features of cells cultured under 3D culture conditions, we analyzed the transcriptomes of bMuSCs cultured in the ACe-gel, alginate, and collagen scaffolds. For biological replicates, bMuSCs obtained from three different cows were used. RNAs were collected after 4 days in the proliferating state and after 8 days in the subsequent differentiation state (Fig. 5A). Among the 34,360 genes identified by sequencing, 9,877 genes with a fold-change (FC) > 1.5 after muscle differentiation in at least one type of scaffold were selected as differentially expressed genes (DEGs). Interestingly, despite the variations among the cell lines from different origins, the principal component analysis (PCA) results for the selected genes revealed that the samples were distinctly clustered depending upon the scaffold type and culture stage (Fig. 5B). These results indicate that overall gene expression in each cell line was commonly influenced by the culture environment, including the scaffold and the medium composition, even in the presence of source-related intrinsic variation.

Next, a clustering heatmap was generated with 418 genes (log<sub>2</sub>(FC)

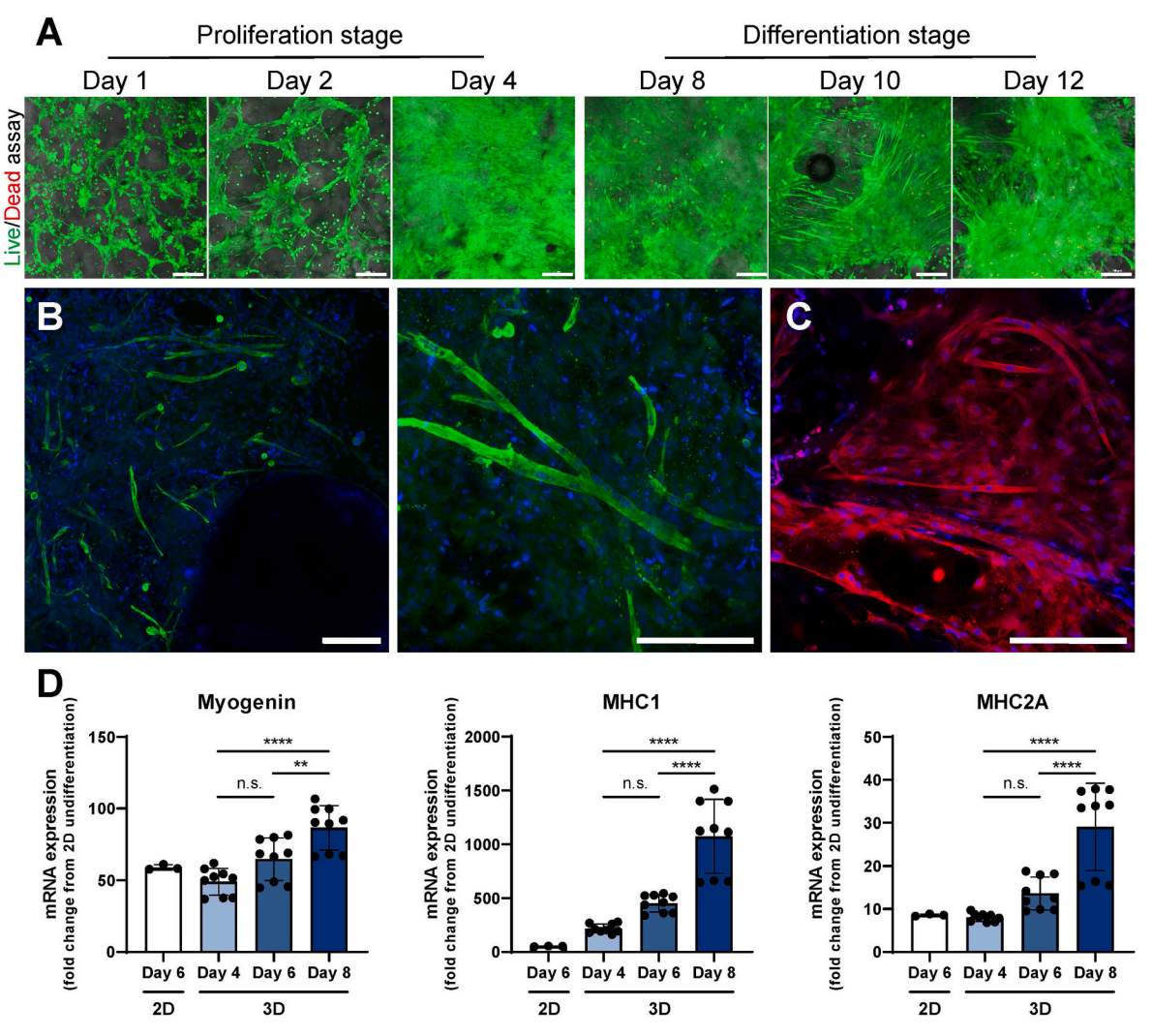


Fig. 4. 3D muscle cell differentiation on the ACe-gel scaffold. (A) Confocal microscopy z-stack imaging of the live/dead assay after proliferation of bMuSCs for 4 days followed by differentiation for 8 days. Scale bars, 200  $\mu$ m. (B–C) Immunofluorescence images of bMuSCs stained for myotube differentiation markers after 8 days of differentiation (Desmin; green, MHC; red) and nuclei (DAPI; blue). Scale bars, 200  $\mu$ m. (D) mRNA expression levels of differentiation-related genes were analyzed using RT–qPCR after 8 days of differentiation. (n.s. > 0.05, \*\*p < 0.01, and \*\*\*\*p < 0.0001).

> 1.5), 226 shared upregulated genes, and 192 shared downregulated genes across three bovine samples after the differentiation stage in the ACe-gel scaffold (Fig. 5C and D). As shown in the PCA plot, the hierarchical clustering of the DEGs showed similarities in stage-associated expression changes regardless of the origin of the bMuSCs. Consistent with the results shown in Fig. 4, the gene ontology (GO) biological process (GOBP) enrichment analysis showed that the upregulated genes in the differentiation stage were mainly associated with muscle cell differentiation and development (Fig. 5E). In contrast, the downregulated genes were associated with processes such as regulation of multicellular organism, system development, positive regulation of biological process, and cellular response to stimulus (Fig. 5F), indicating that the cells might have achieved a state of stability in the differentiation stage, potentially minimizing unnecessary changes or developmental processes.

Furthermore, to understand the differences in environmental effects between scaffolds, we also compared the RNA expression profiles of cells cultured in the ACe-gel scaffold with those of cells cultured in other scaffolds. Based on a Venn diagram representing the number of genes that were up- or downregulated between scaffolds during the growth or differentiation stage, GOBP analysis was performed (Supple. Figs. S12A and B). Notably, the upregulated genes in the ACe-gel scaffold compared to the other scaffolds were associated with muscle cell or tissue

development in both the growth and differentiation stages (Supple. Figs. S12C-F). The downregulated genes in the ACe-gel scaffold compared to the collagen scaffold in the proliferation phase were mainly associated with cellular proliferation (Supple. Fig. S12G). In the differentiation phase, genes that were expressed at lower levels in the ACe-gel scaffold than in collagen scaffold were primarily associated with the cholesterol biosynthetic process (Supple. Fig. S12H). This suggests that the animal-derived collagen scaffold has an advantage in cell growth, even though the ACe-gel scaffold also offered a comparable cell proliferation environment. In a comparison with the alginate scaffold, the downregulated genes in the ACe-gel scaffolds were related to inflammatory or immune responses during the proliferation stage as well as the differentiation stage, indicating that the pure alginate scaffold generates a more stressful environment for cell growth (Supple. Figs. S12I and J). Overall, the findings from the transcriptomic analysis suggest that the ACe-gel scaffold offers a conducive environment for muscle cell culture and differentiation, confirming its suitability for applications in cultivated meat.

#### 3.5. The ACe-gel can be applied to cultivate meat as food

The ACe-gel scaffold can be manufactured in a variety of shapes, even in a shape similar to a single piece of steak. After the cells were H. Lee et al. Food Hydrocolloids 152 (2024) 109944

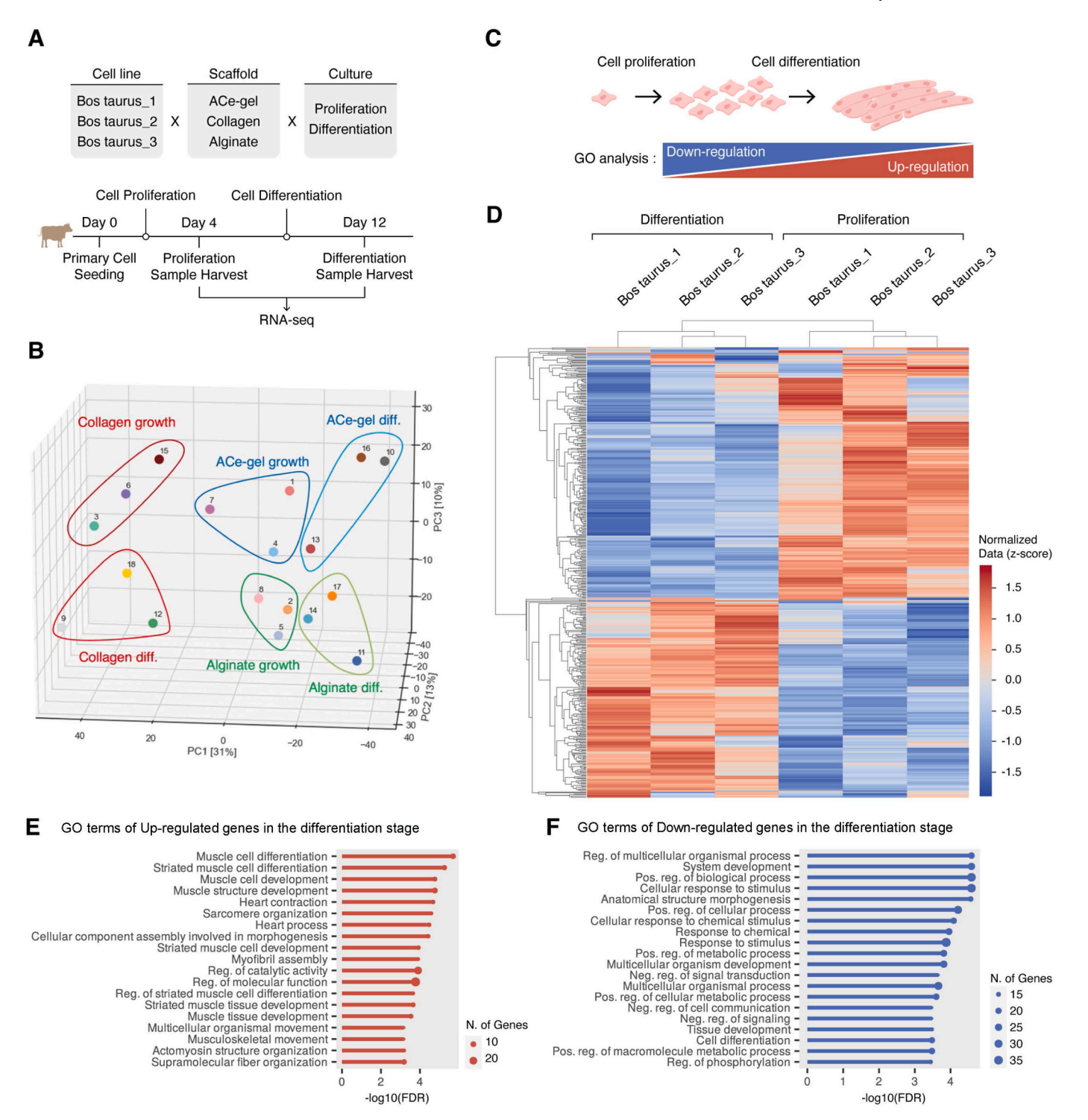


Fig. 5. Comprehensive RNA sequencing analysis exhibiting enhanced muscle differentiation in the ACe-gel scaffold. (A) Experimental design of sample preparation. (B) Principal component analysis (PCA) of RNA sequencing, grouped according to culture conditions. (C) Scheme of Gene Ontology (GO) term analysis for downregulated (blue) and upregulated (red) DEGs induced by differentiation within the ACe-gel scaffold. (D) Clustering heatmap of the DEGs during the proliferation and differentiation stage in the ACe-gel scaffold. (E, F) GO term analysis of upregulated (E) or downregulated (F) genes at the end of the differentiation phase in the ACe-gel scaffold.

cultured on the lyophilized ACe-gel scaffold, the prototype cultivated meat had a color similar to that of fresh beef after staining in 2% Monascus pigment solution (Fig. 6A). In addition, cooking properties and sensory acceptability with the prototype ACe-gel-based cultivated meat were tested. Even after panfrying, structural disintegration or degradation was not observed in the centimeter-thick cultivated meat (Fig. 6B). The textural characteristics measured by the stress-strain

curve revealed that both cultivated meat and beef exhibited increased stress and compressive modulus values after cooking. The Young's modulus of cultivated meat with the ACe-gel rose from 285.19  $\pm$  83.37 kPa in the raw state to 880.60  $\pm$  485.60 kPa after cooking, while the modulus of beef increased from 267.76  $\pm$  156.42 kPa in its raw state to 1331.94  $\pm$  762.43 kPa after cooking (Fig. 6C and D). Of note, to minimize variability during the cooking process, cultured meat and raw beef

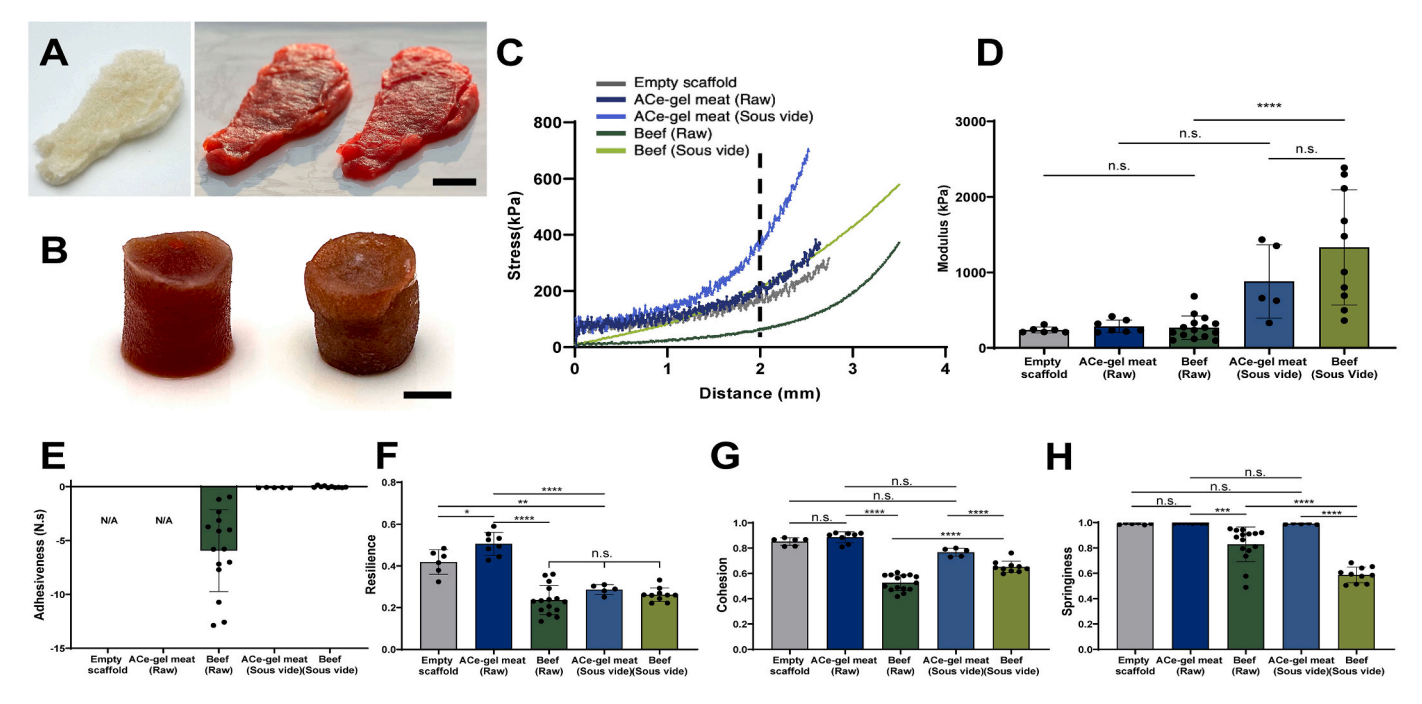


Fig. 6. The ACe-gel scaffold application in cultivated meat as a food. (A) Steak-shaped lyophilized ACe-gel scaffold (left) and steak-shaped cultivated meat (right); scale bar: 2 cm. (B) Cultivated meat before cooking (left) and after panfrying (right); scale bar: 5 mm. (C) Stress-strain curve of cultivated meat and beef according to the compression distance. (D–H) The corrected compressive modulus (D), adhesiveness (E), resilience (F), cohesion (G), and springiness (H) of cultivated meat and beef.

of the same size were cooked with a sous vide approach.

The adhesiveness of both the empty scaffold and the cultivated meat raw sample was undetectable, likely indicative of the intrinsic properties of the scaffold (Fig. 6E). The resilience and cohesion values of the cooked ACe-gel meat were 0.29  $\pm$  0.02 and 0.77  $\pm$  0.03, respectively, which closely resembled those of cooked beef (resilience:  $0.26 \pm 0.03$ and cohesion:  $0.65 \pm 0.05$ ). This provides additional evidence of the scaffold's ability to maintain its textural attributes following thermal treatment (Fig. 6F and G). The scaffold exhibited a high level of springiness, possibly attributed to its elevated moisture content and porosity, and this characteristic remained consistent both before and after cooking with the ACe-gel scaffold (Fig. 6H). The ACe-gel-based cultivated meat has not yet fully matched beef, which would be needed for co-culturing with other cell types, including adipose cells, and post-processing. Nevertheless, these findings suggest that the scaffold has the potential to emulate the chewiness and mouthfeel associated with traditional meat.

Generally, seaweed has a distinct flavor. In U. pinnatifida, compounds such as  $\beta$ -ionone, pentadecane, 2-methylnonane, hexadecane, heptadecane, butane, benzaldehyde, hexanal, and 2-heptenal are known to contribute to a unique odor (Coleman, et al., 2022; Garicano Vilar, O'Sullivan, Kerry, & Kilcawley, 2020). Given the possibility that these fishy odors could persist in the manufacturing process and influence the flavor of the cultured meat, the seven main odor-active compounds were

measured in *U. pinnatifida* and the ACe-gel via electronic nose analysis. Interestingly, significant reductions in the tested chemicals were observed in the ACe-gel compared to *U. pinnatifida* (Table 1), indicating that compounds inducing fishy odors would be washed out during the ACe-gel production process.

Brown algae are known to adsorb a significant amount of heavy metals in marine environments (Davis, Volesky, & Mucci, 2003). Since the ACe-gel scaffold is produced physically from seaweed and cultivation with scaffolds does not involve any specific heavy metal removal process, it is possible that heavy metals may still be present in the scaffold. For safety testing for food application, the heavy metal contents were measured in harvested *U. pinnatifida*, commercial alginate, and the ACe-gel (Supple. Fig. S13). The results showed that heavy metals such as copper, cadmium, lead, tin, and arsenic were present at levels compliant with food regulations in *U. pinnatifida*. However, these metals were hardly detected in commercial alginate and the ACe-gel. Overall, the ACe-gel scaffold is not only a suitable biological material for cell culture but also appropriate for application and consumption in foods.

## 4. Discussion

As global risks have called into question the sustainability of our current protein consumption system, the development of cultivated meat has become crucial. However, there are numerous technical

 Table 1

 Comparison of the electronic-nose chromatogram peak areas of odor-active compounds for *U. pinnatifida* and the ACe-gel.

| Peak area of intensity (relative) |                 |                      |           |           |           |           |           |           |
|-----------------------------------|-----------------|----------------------|-----------|-----------|-----------|-----------|-----------|-----------|
| Odor-active compound              |                 | Retention Time (sec) | Seaweed 1 | Seaweed 2 | Seaweed 3 | ACe-gel 1 | ACe-gel 2 | ACe-gel 3 |
| Hydrocarbons                      | 2-Methylnonane  | 98.92–100.72         | 2854.8    | 2157.8    | 2503.3    | 248.1     | 213.9     | 217.4     |
| -                                 | Hexadecane      | 163.79-163.83        | 398.1     | 322.2     | 324.2     | N/A       | N/A       | N/A       |
|                                   | Heptadecane     | 171.52-171.77        | 194.9     | 127.2     | 77.1      | 56        | 82.5      | N/A       |
|                                   | Pentadecane     | 157.53-158.34        | 746.5     | 205.2     | 439.1     | 166.6     | 87.1      | 152.2     |
| Ketones                           | $\beta$ -Ionone | 158.12-158.34        | 180.8     | 130.8     | 233.7     | 166.6     | 362.4     | 586.7     |
| Aldehydes                         | Benzaldehyde    | 99.02-103.84         | 28516.9   | 18577.3   | 12972.3   | 248.1     | 610.2     | 636.6     |
|                                   | Hexanal         | 52.45-54.34          | 8025.5    | 50306.1   | 59698.9   | 1754      | 1526.6    | 1588.8    |

difficulties related to this development process, including mass production of steak-like meat at a reasonable cost. Accordingly, developing an appropriate scaffold is essential to overcome these difficulties. From a biological standpoint, the scaffold must provide an effective 3D environment for cell growth and differentiation, as well as cultivation in a thick conformation. From an industrial perspective, the scaffold must meet various standards, including standards for consistency, reproducibility, shelf life, availability of raw material, possibility of mass production, and sensory properties as a food for commercialization. Many research groups and companies are even exploring scaffold-free strategies or developing scaffold removal technologies for scalable production, emphasizing the critical role of scaffolding solutions in the cultivated meat industry (Ahmad, et al., 2021; Ye, Zhou, Guan, & Sun, 2022). In this study, we developed the ACe-gel scaffold from brown algae as a non-animal-based scaffold, and this approach is suitable for producing cultivated meat without a removal process.

Cell adhesion is crucial, as it is the initiating event for subsequent proliferation and stable differentiation. Compared to pure alginate, which makes cell adhesion on the scaffold challenging, the ACe-gel scaffold has several distinguishing features, including cell adhesion and proliferation. The ACe-gel is composed mainly of alginate, which accounts for approximately 60% of the total content. Beyond alginate, seaweeds contain significant amounts of various glycoproteins, including fucoidan, proteins, halide compounds, and other ions, and these compounds can support cell adhesion (Mazeas, et al., 2023), which might contribute to cell adhesion in the ACe-gel scaffolds. Another interesting aspect of the ACe-gel is its nanotopographical characteristics. The nanotopography of the scaffold surface has recently attracted much attention in the context of 3D cell culture because it can influence cell-matrix and cell-cell interactions, aiding in cell alignment (Arnold, et al., 2004; Ben-Arye, et al., 2020). Further research is needed to determine whether alginate-based nanodots provide distinct cell adhesion properties compared to smooth alginate surfaces. Considering the significant upregulation of genes associated with cellular stress during growth in commercial alginate, it is evident that the cell-scaffold (matrix) interaction is crucial in the 3D cell culture system.

To design a 3D cell culture system, including systems for application in the production of cultivated meats, the diffusion of oxygen and nutrients and the removal of waste throughout the structure are critical for cell survival in the scaffold with a thick conformation (Enrione, et al., 2017; Griffith et al., 2005; D. Kim et al., 2022). The uniformly distributed porous structure of the ACe-gel scaffold could contribute to the efficient diffusion of nutrients and oxygen into the structure in 3D cell culture, even with a thickness in the centimeter range. Moreover, the ACe-gel uniquely maintained the trumpet-hypha network in *U. pinnatifida*, which could serve a function akin to blood vessels in the scaffold, although the detailed function of the hypha network in the ACe-gel in maintaining cells beyond cell adhesion must be determined in the future. Notably, genes associated with hypoxia-related or cellular stress factors were not classified as gene ontology terms in the ACe-gel-based culture condition.

In terms of food safety, the ACe-gel scaffold for cultivated meats has several key features for application. To culture animal cells in plant or animal tissues, they generally undergo a process called decellularization (Adamski, et al., 2018; Gilpin & Yang, 2017; Jones, Rebello, & Gaudette, 2021; Modulevsky, Lefebvre, Haase, Al-Rekabi, & Pelling, 2014). For decellularization, surfactants such as sodium dodecyl sulfate are typically used, which is more of a biological issue for the culture of cells rather than a food issue. Moreover, there are multiple limitations, including food approval, related to the use of detergents as additives in food. Notably, the ACe-gel is manufactured using a physical extraction method, thereby negating any food safety concerns associated with the production process. Our research discovered that removing residual proteins and DNA from the original tissues is unnecessary when developing cultured products. In other words, if scaffolds for cell culture were initially created as an edible material without cellular toxicity, they

could be considered applicable for cultivated meat production even without a decellularization process. Moreover, even the ACe-gel is a material originating from seaweed, the potential risks of heavy metals could be minimized because the scaffold is fabricated solely from the medullar region of seaweed after removing the outer cortex. As a result, the levels of heavy metals in the ACe-gel were virtually undetectable, ensuring its safety for food consumption. Regarding the sensory of food, the ACe-gel also exhibited significantly reduced levels of odor-active compounds.

Practically, the raw material of the ACe-gel can be obtained in large quantities from the ocean at low cost, and the fabrication of the extract is relatively simple. Therefore, the ACe-gel scaffold could be advantageous for mass production. Applying this to a conventional suspension bioreactor for upscaling is the next step toward mass production of the cultivated meat. Furthermore, it is waiting to test the conditions for co-culturing cells composing muscle, such as adipocytes and fibroblasts, in the ACe-gel for developing cultivated meat. Beyond its application in cultivated meat, the ACel-gel has structural versatility, enabling its production in various forms, such as thick scaffolds, microcarriers, and bead-type matrices. This adaptability could allow its application in diverse conditions where 3D cell culture is needed.

#### 5. Conclusions

The brown alga-derived ACe-gel scaffold, which is animal-free, provides a suitable environment for cell culture, promoting the growth and differentiation of muscle cells. Therefore, the ACe-gel is expected to become a commercial-grade material that can be used in food biotechnology to produce cultivated meat, which requires cells to be grown and differentiated. The results of this study demonstrate the potential usage of the ACe-gel in 3D cell culture technology, not only for the culture of muscle cells for cultivated meat but also for various types of cells, providing significant opportunities for cell-based medical and life science research.

## CRediT authorship contribution statement

Heejae Lee: Conceptualization, Data curation, Formal analysis, Visualization, Funding acquisition, Investigation, Project administration, Supervision, Validation, Writing - original draft. Dasom Kim: Data curation, Formal analysis, Validation. Kyeong Hun Choi: Data curation, Formal analysis, Visualization, Validation. Sangmin Lee: Data curation, Formal analysis, Validation. Minguk Jo: Data curation, Formal analysis, Validation. Song-Yi Chun: Data curation, Formal analysis, Validation. Yebin Son: Data curation, Formal analysis, Validation. Jong Ha Lee: Data curation, Formal analysis, Validation. Kwanhyeong Kim: Data curation, Formal analysis, Validation. TaeByung Lee: Data curation, Formal analysis, Validation. Joonho Keum: Conceptualization. Min Yoon: Data curation, Formal analysis, Validation. Hyung Joon Cha: Data curation, Formal analysis, Supervision. Sangchul Rho: Data curation, Formal analysis, Supervision. Sung Chun Cho: Funding acquisition, Investigation, Project administration, Validation, Writing original draft, Writing - review & editing. Young-Sam Lee: Supervision, Writing - original draft, Writing - review & editing.

# Declaration of competing interest

The authors declare the following financial interests/personal relationships which may be considered as potential competing interests:

H. Lee, D. Kim, K.H. Choi, S. Chun, Y. Son, J.H. Lee, K. Kim, T.B. Lee, M. Yoon, and S.C. Cho are employees of SeaWith Inc. (S. Korea), which funded this research. H. Lee is the chief technology officer and a shareholder, and S.C. Cho is the research and development director and a shareholder of SeaWith Inc. SeaWith Inc. holds a patent (KR 10–2151203) related to the technology and methodology presented in this paper. Additionally, the company has pending patent applications,

including KR 10-2022-0065408, PCT/KR2022/007575, US 17/771,459, and EU 20902919.8, concerning the technology and methodology described in this article. The authors declare no other potential conflicts of interest with respect to the research, authorship, and/or publication of this article.

#### Data availability

H. Lee et al.

Data will be made available on reasonable request.

#### Acknowledgments

We thank Professor Ki Yong Chung from the Korea National College of Agriculture and Fisheries for kindly providing the bMuSCs. We also extend our gratitude to Harim Jang, a doctoral candidate at Seoul National University, for her invaluable assistance in generating the figures. This work was supported by the Korea Institute of Planning and Evaluation for Technology in Food, Agriculture and Forestry (IPET) through the High Value-added Food Technology Development Program, funded by the Ministry of Agriculture, Food and Rural Affairs (MAFRA) (321025-05), and the Korea Institute of Marine Science & Technology Promotion (KIMST) funded by the Ministry of Oceans and Fisheries (00245016).

#### Appendix A. Supplementary data

Supplementary data to this article can be found online at https://doi.org/10.1016/j.foodhyd.2024.109944.

#### References

- Adamski, M., Fontana, G., Gershlak, J. R., Gaudette, G. R., Le, H. D., & Murphy, W. L. (2018). Two methods for decellularization of plant tissues for tissue engineering applications. *Journal of Visualized Experiments: JoVE, 135*, Article e57586.
- Ahmad, K., Lim, J. H., Lee, E. J., Chun, H. J., Ali, S., Ahmad, S. S., et al. (2021). Extracellular matrix and the production of cultured meat. *Foods*, *10*(12), 3116.
- Alexandratos, N., & Bruinsma, J. (2012). World agriculture towards 2030/2050: The 2012
- Andersen, T., Auk-Emblem, P., & Dornish, M. (2015). 3D cell culture in alginate hydrogels. *Microarrays*, 4(2), 133–161.
- Arnold, M., Cavalcanti-Adam, E. A., Glass, R., Blummel, J., Eck, W., Kantlehner, M., et al. (2004). Activation of integrin function by nanopatterned adhesive interfaces. *ChemPhysChem*, 5(3), 383–388.
- Bar-Shai, N., Sharabani-Yosef, O., Zollmann, M., Lesman, A., & Golberg, A. (2021). Seaweed cellulose scaffolds derived from green macroalgae for tissue engineering. Scientific Reports, 11(1), Article 11843.
- Ben-Arye, T., & Levenberg, S. (2019). Tissue engineering for clean meat production. Frontiers in Sustainable Food Systems, 3, 46.
- Ben-Arye, T., Shandalov, Y., Ben-Shaul, S., Landau, S., Zagury, Y., Ianovici, I., et al. (2020). Textured soy protein scaffolds enable the generation of three-dimensional bovine skeletal muscle tissue for cell-based meat. *Nature Food*, 1(4), 210–220.
- Bhat, Z. F., Morton, J. D., Mason, S. L., Bekhit, A. E. A., & Bhat, H. F. (2019). Technological, regulatory, and ethical aspects of in vitro meat: A future slaughter-free harvest. Comprehensive Reviews in Food Science and Food Safety, 18(4), 1192–1208.
- Bomkamp, C., Musgrove, L., Marques, D. M. C., Fernando, G. F., Ferreira, F. C., & Specht, E. A. (2023). Differentiation and maturation of muscle and fat cells in cultivated seafood: Lessons from developmental biology. *Marine Biotechnology*, 25 (1), 1–29.
- Bomkamp, C., Skaalure, S. C., Fernando, G. F., Ben-Arye, T., Swartz, E. W., & Specht, E. A. (2022). Scaffolding biomaterials for 3D cultivated meat: Prospects and challenges. Advanced Science, 9(3), Article e2102908.
- Campuzano, S., & Pelling, A. E. (2019). Scaffolds for 3D cell culture and cellular agriculture applications derived from non-animal sources. Frontiers in Sustainable Food Systems, 3, 38.
- Choudhury, D., Tseng, T. W., & Swartz, E. (2020). The business of cultured meat. Trends in Biotechnology, 38(6), 573–577.
- Coleman, B., Van Poucke, C., Dewitte, B., Ruttens, A., Moerdijk-Poortvliet, T., Latsos, C., et al. (2022). Potential of microalgae as flavoring agents for plant-based seafood alternatives. Future Foods, 5, Article 100139.
- Davis, T. A., Volesky, B., & Mucci, A. (2003). A review of the biochemistry of heavy metal biosorption by brown algae. *Water Research*, 37(18), 4311–4330.
- de Las Heras-Saldana, S., Chung, K. Y., Lee, S. H., & Gondro, C. (2019). Gene expression of Hanwoo satellite cell differentiation in longissimus dorsi and semimembranosus. BMC Genomics, 20(1), 156.

- Enrione, J., Blaker, J. J., Brown, D. I., Weinstein-Oppenheimer, C. R., Pepczynska, M., Olguin, Y., et al. (2017). Edible scaffolds based on non-mammalian biopolymers for myoblast growth. *Materials*, 10(12), 1404.
- Estrada-Villegas, G., Morselli, G., Oliveira, M., Gonzalez-Perez, G., & Lugão, A. (2020). PVGA/Alginate-AgNPs hydrogel as absorbent biomaterial and its soil biodegradation behavior. *Polymer Bulletin*, 77(8), 4147–4166.
- Fajardo, A. R., Silva, M. B., Lopes, L. C., Piai, J. F., Rubira, A. F., & Muniz, E. C. (2012). Hydrogel based on an alginate–Ca 2+/chondroitin sulfate matrix as a potential colon-specific drug delivery system. RSC Advances, 2(29), 11095–11103.
- Fraeye, I., Kratka, M., Vandenburgh, H., & Thorrez, L. (2020). Sensorial and nutritional aspects of cultured meat in comparison to traditional meat: Much to Be inferred. Frontiers in Nutrition. 7, 35.
- Freed, L. E., Vunjak-Novakovic, G., Biron, R. J., Eagles, D. B., Lesnoy, D. C., Barlow, S. K., et al. (1994). Biodegradable polymer scaffolds for tissue engineering. *Biotechnology*, 12(7), 689–693.
- Garicano Vilar, E., O'Sullivan, M. G., Kerry, J. P., & Kilcawley, K. N. (2020). Volatile compounds of six species of edible seaweed: A review. *Algal Research*, 45, Article 101740.
- Gilpin, A., & Yang, Y. (2017). Decellularization strategies for regenerative medicine: From processing techniques to applications. BioMed Research International, 2017, Article 9831534
- Griffith, C. K., Miller, C., Sainson, R. C., Calvert, J. W., Jeon, N. L., Hughes, C. C., et al. (2005). Diffusion limits of an in vitro thick prevascularized tissue. *Tissue Engineering*, 11(1–2), 257–266.
- Haycock, J. W. (2011). 3D cell culture: A review of current approaches and techniques. Methods in Molecular Biology, 695, 1–15.
- Hoek, C., Mann, D., Jahns, H. M., & Jahns, M. (1995). Algae: An introduction to phycology. Cambridge university press.
- Ianovici, I., Zagury, Y., Redenski, I., Lavon, N., & Levenberg, S. (2022). 3D-printable plant protein-enriched scaffolds for cultivated meat development. *Biomaterials*, 284, Article 121487.
- Im, Y.-G., Choi, J.-S., & Kim, D.-S. (2006). Mineral contents of edible seaweeds collected from Gijang and Wando in Korea. Korean Journal of Fisheries and Aquatic Sciences, 39, 16–22.
- Jensen, H. M., Larsen, F. H., & Engelsen, S. B. (2015). Characterization of alginates by nuclear magnetic resonance (NMR) and vibrational spectroscopy (IR, NIR, Raman) in combination with chemometrics. *Methods in Molecular Biology*, 1308, 347–363.
- Jeong, D., Seo, J. W., Lee, H. G., Jung, W. K., Park, Y. H., & Bae, H. (2022). Efficient myogenic/adipogenic transdifferentiation of bovine fibroblasts in a 3D bioprinting system for steak-type cultured meat production. *Advanced Science*, 9(31), Article e2202877.
- Jin, Y., Jeon, E. J., Jeong, S., Min, S., Choi, Y. S., Kim, S. H., et al. (2021). Reconstruction of muscle fascicle-like tissues by anisotropic 3D patterning. Advanced Functional Materials, 31(25), Article 2006227.
- Jithendra, P., Rajam, A. M., Kalaivani, T., Mandal, A. B., & Rose, C. (2013). Preparation and characterization of aloe vera blended collagen-chitosan composite scaffold for tissue engineering applications. ACS Applied Materials & Interfaces, 5(15), 7291–7298
- Jones, J. D., Rebello, A. S., & Gaudette, G. R. (2021). Decellularized spinach: An edible scaffold for laboratory-grown meat. Food Bioscience, 41, Article 100986.
- Kang, D. H., Chung, K. Y., Park, B. H., Kim, U. H., Jang, S. S., Smith, Z. K., et al. (2022). Effects of feeding high-energy diet on growth performance, blood parameters, and carcass traits in Hanwoo steers. *Anim Biosci*, 35(10), 1545–1555.
- Kang, D. H., Louis, F., Liu, H., Shimoda, H., Nishiyama, Y., Nozawa, H., et al. (2021). Engineered whole cut meat-like tissue by the assembly of cell fibers using tendon-gel integrated bioprinting. *Nature Communications*, 12(1), 5059.
- Kim, D., Hwang, K. S., Seo, E. U., Seo, S., Lee, B. C., Choi, N., et al. (2022). Vascularized lung cancer model for evaluating the promoted transport of anticancer drugs and immune cells in an engineered tumor microenvironment. *Advanced Healthcare Materials*, 11(12), Article e2102581.
- Kim, C.-J., Kim, S.-H., Lee, E.-Y., Son, Y.-M., Bakhsh, A., Hwang, Y.-H., et al. (2023). Optimal temperature for culturing chicken satellite cells to enhance production yield and umami intensity of cultured meat. Food Chemistry Advances, 2, Article 100307.
- Komiya, Y., Mizunoya, W., Kajiwara, K., Yokoyama, I., Ogasawara, H., & Arihara, K. (2020). Correlation between skeletal muscle fiber type and responses of a taste sensing system in various beef samples. *Animal Science Journal*, 91(1), Article e13425.
- Koo, J.-G. (2020). Chemical composition and rheological properties of polysaccharides isolated from different parts of Brown seaweed Undaria pinnatifida. Korean Journal of Fisheries and Aquatic Sciences, 53(5), 665–671.
- Lee, J. T., & Chow, K. L. (2012). SEM sample preparation for cells on 3D scaffolds by freeze-drying and HMDS. Scanning, 34(1), 12–25.
- Lee, J., Cuddihy, M. J., & Kotov, N. A. (2008). Three-dimensional cell culture matrices: State of the art. Tissue Engineering. Part B: Reviews, 14(1), 61–86.
- Lee, K. Y., Loh, H. X., & Wan, A. C. A. (2021). Systems for muscle cell differentiation: From bioengineering to future food. *Micromachines*, 13(1), 71.
- Lee, K. Y., & Mooney, D. J. (2012). Alginate: Properties and biomedical applications. Progress in Polymer Science, 37(1), 106–126.
- Lee, M., Wu, B. M., & Dunn, J. C. (2008). Effect of scaffold architecture and pore size on smooth muscle cell growth. *Journal of Biomedical Materials Research Part A*, 87(4), 1010–1016.
- Li, J., Fang, W., Hao, T., Dong, D., Yang, B., Yao, F., et al. (2020). An anti-oxidative and conductive composite scaffold for cardiac tissue engineering. *Composites Part B: Engineering*, 199, Article 108285.
- Li, C. H., Yang, I. H., Ke, C. J., Chi, C. Y., Matahum, J., Kuan, C. Y., et al. (2022). The production of fat-containing cultured meat by stacking aligned muscle layers and

- adipose layers formed from gelatin-soymilk scaffold. Frontiers in Bioengineering and Biotechnology, 10, Article 875069.
- Lin, Y. M., Lee, J., Lim, J. F. Y., Choolani, M., Chan, J. K. Y., Reuveny, S., et al. (2017). Critical attributes of human early mesenchymal stromal cell-laden microcarrier constructs for improved chondrogenic differentiation. Stem Cell Research & Therapy, 8(1), 93.
- Liu, Y., Wang, R., Ding, S., Deng, L., Zhang, Y., Li, J., et al. (2022). Engineered meatballs via scalable skeletal muscle cell expansion and modular micro-tissue assembly using porous gelatin micro-carriers. *Biomaterials*, 287, Article 121615.
- MacQueen, L. A., Alver, C. G., Chantre, C. O., Ahn, S., Cera, L., Gonzalez, G. M., et al. (2019). Muscle tissue engineering in fibrous gelatin: Implications for meat analogs. NPJ Sci Food. 3, 20.
- Mazeas, L., Yonamine, R., Barbeyron, T., Henrissat, B., Drula, E., Terrapon, N., et al. (2023). Assembly and synthesis of the extracellular matrix in brown algae. Seminars in Cell & Developmental Biology, 134, 112–124.
- Modulevsky, D. J., Lefebvre, C., Haase, K., Al-Rekabi, Z., & Pelling, A. E. (2014). Apple derived cellulose scaffolds for 3D mammalian cell culture. PLoS One, 9(5), Article 20725.
- Nishide, E., Kinoshita, Y., Anzai, H., & Uchida, N. (1988). Distribution of hot-water extractable material, water-soluble alginate and alkali-soluble alginate in different parts of <i>Undaria pinnatifida</ii&gt. Nippon Suisan Gakkaishi, 54(9), 1619–1622.</p>
- Rowley, J. A., Madlambayan, G., & Mooney, D. J. (1999). Alginate hydrogels as synthetic extracellular matrix materials. *Biomaterials*, 20(1), 45–53.
- Rupérez, P., & Saura-Calixto, F. (2001). Dietary fibre and physicochemical properties of edible Spanish seaweeds. European Food Research and Technology, 212(3), 349–354.
- Salisu, A., Sanagi, M. M., Abu Naim, A., Abd Karim, K. J., Wan Ibrahim, W. A., & Abdulganiyu, U. (2016). Alginate graft polyacrylonitrile beads for the removal of lead from aqueous solutions. *Polymer Bulletin*, 73, 519–537.
- Schmitz, K., & Srivastava, L. M. (1976). The fine structure of sieve elements of nereocystis lutkeana. American Journal of Botany, 63(5), 679–693.
- Sharma, S., Thind, S. S., & Kaur, A. (2015). In vitro meat production system: Why and how? *Journal of Food Science & Technology*, 52(12), 7599–7607.
- Stabler, C., Wilks, K., Sambanis, A., & Constantinidis, I. (2001). The effects of alginate composition on encapsulated  $\beta$ TC3 cells. *Biomaterials*, 22(11), 1301–1310.

- Sun, H., Hu, C., Zhou, C., Wu, L., Sun, J., Zhou, X., et al. (2020). 3D printing of calcium phosphate scaffolds with controlled release of antibacterial functions for jaw bone repair. *Materials & Design*, 189, Article 108540.
- Szekalska, M., Pucitowska, A., Szymańska, E., Ciosek, P., & Winnicka, K. (2016).
  Alginate: Current use and future perspectives in pharmaceutical and biomedical applications. *International Journal of Polymer Science*, 2016, 1–17.
- Tsai, A. C., Jeske, R., Chen, X., Yuan, X., & Li, Y. (2020). Influence of microenvironment on mesenchymal stem cell therapeutic potency: From planar culture to microcarriers. Frontiers in Bioengineering and Biotechnology, 8, 640.
- van der Weele, C., & Tramper, J. (2014). Cultured meat: Every village its own factory? Trends in Biotechnology, 32(6), 294–296.
- Ververis, C., Georghiou, K., Danielidis, D., Hatzinikolaou, D. G., Santas, P., Santas, R., et al. (2007). Cellulose, hemicelluloses, lignin and ash content of some organic materials and their suitability for use as paper pulp supplements. *Bioresource Technology*, 98(2), 296–301.
- Weller, R. F., Marley, C. L., & Moorby, J. M. (2007). Effects of organic and conventional feeding regimes and husbandry methods on the quality of milk and dairy products. In *Handbook of organic food safety and quality* (pp. 97–116). Elsevier.
- Wheeler, T., & Braun, J.v. (2013). Climate change impacts on global food security. Science, 341(6145), 508–513.
- Xiang, N., Yuen, J. S. K., Jr., Stout, A. J., Rubio, N. R., Chen, Y., & Kaplan, D. L. (2022).
  3D porous scaffolds from wheat glutenin for cultured meat applications. *Biomaterials*, 285, Article 121543.
- Yan, Q., Fei, Z., Li, M., Zhou, J., Du, G., & Guan, X. (2022). Naringenin promotes myotube formation and maturation for cultured meat production. *Foods*, 11(23), 3755
- Yang, J., Guertin, P., Jia, G., Lv, Z., Yang, H., & Ju, D. (2019). Large-scale microcarrier culture of HEK293T cells and Vero cells in single-use bioreactors. AMB Express, 9(1), 70
- Ye, Y., Zhou, J., Guan, X., & Sun, X. (2022). Commercialization of cultured meat products: Current status, challenges, and strategic prospects. *Future Foods*, 6, Article 100177.
- Zeltinger, J., Sherwood, J. K., Graham, D. A., Müeller, R., & Griffith, L. G. (2001). Effect of pore size and void fraction on cellular adhesion, proliferation, and matrix deposition. *Tissue Engineering*, 7(5), 557–572.